PROCEEDINGS OF THE 16th SYMPOSIUM ON THE GEOLOGY OF THE BAHAMAS AND OTHER CARBONATE REGIONS

Edited by

Bosiljka Glumac and Michael Savarese

Gerace Research Centre

San Salvador, Bahamas

2016

Cover photo: San Salvador coastline photo by Erin Rothfus.

Press: A & A Printing

PRELIMINARY GEOPHYSICAL CHARACTERIZATION OF THE KARST WITHIN A TRANSVERSE GLADE IN THE ATLANTIC COASTAL RIDGE, MIAMI-DADE COUNTY FLORIDA, USA

Lee J. Florea[a*], Jeff Ransom[b], and Dallas Hazelton[b]

[a] Department of Geological Sciences, Ball State University
Muncie, IN 47306 (USA)
[b] Natural Areas Management, Miami-Dade County Parks, Recreation, and Open Spaces
Miami, FL 33170

ABSTRACT. In this paper we present results of two DC Electrical Resistivity Tomography surveys at Deering Estate at Cutler in the Atlantic Coastal Ridge of Miami-Dade County, Florida. This County Natural Area encompasses Deering Glade and hosts one of the largest remaining tropical hardwood-hammock ecosystems in the USA. A canal extension, wetland restoration, and pump station recently constructed at Deering Estate by the South Florida Water Management District is designed to re-hydrate Deering Glade to pre-development conditions thus helping to sustain the hammock ecosystem and reverse trends in salt-water intrusion in this portion of the Biscayne aquifer.

For these transects, we used an AGI Super Sting R1/IP with an array of 28 passive electrodes used in a dipole-dipole configuration. The first transect comprised a 46-m 'roll-along' survey from the glade interior across the north scarp. In this transect, we used one-meter electrode spacing with a 10-electrode overlap between the two segments. In the second transect, we spanned the glade using a 5-m spacing for a 112-m-long transect. Our first and second transects 'see' to a depth of approximate 9 m and 27 m below modern sea level, respectively.

In our inversion from the first transect, we clearly identify the high-resistivity vadose zone north of the glade scarp and identify a high-resistivity anomaly that is likely an air-filled cave and aligns with the SW-NE trend of surveyed caves in the northern glade margin. In the inversion from the second transect, the vadose zone in the north scarp is still visible. The southern margin of the glade is highly dissected by excessive root wedging and tree throw, resulting in greater hydration and lower resistivity. A low-resistivity anomaly below the center of the glade potentially represents a cave filled with fresh groundwater. An increase in resistivity at depth potentially represents the contact between the massive permeability of *Ophiomorpha* ichnofabric in the MIS 5e Miami Limestone and occluded touching-vug porosity in the older carbonates of the Pleistocene Ft. Thompson Formation.

*Corresponding author. E-mail: lflorea@bsu.edu

INTRODUCTION

Physical and Geological Setting

The Deering Estate at Cutler (a unit of Miami-Dade County Natural and Historic Preserve) includes one of the largest remaining tracts of tropical hardwood hammock that once dominated the landscape along the Atlantic Coastal Ridge in southeast Florida, USA. A thin soil cover characterizes the hammock, with exposed rock pinnacles, shallow sinkholes, and dense vegetation acclimated to the monsoonal nature of rainfall (annual average 1.25–1.5 m) with long periods of xeric conditions in the winter and spring. Common hardwoods include Gumbo Limbo, Poisonwood, Live Oak, and varieties of *Ficus*. Ferns and various epiphytes grow thick in the understory. On average the coastal ridge is 3–5 m with maximum elevation of 7.3 m above modern sea level (Hoffemeister et al., 1967).

A low elevation glade divides this hammock. Prior to development and the reduction
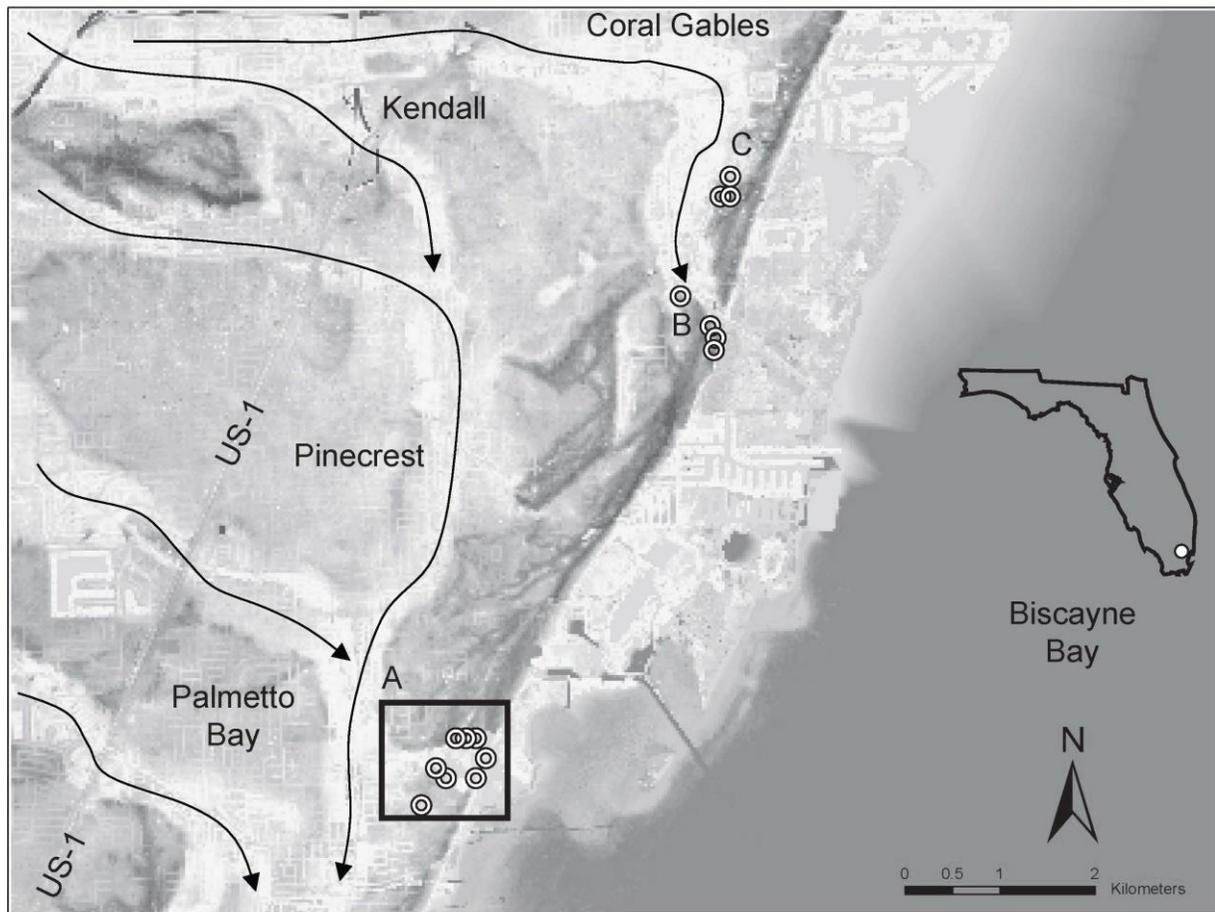
Figure 1. LiDAR map of elevations in a portion of the Atlantic Coastal Ridge in Miami-Dade County, Florida (LiDAR data form the South Florida Water Management District). The geomorphic structure of the tidal-barrier-bar system is visible. Historic directions of surface water flow within glades are indicated by arrows. Caves are shown by open circles. A) Deering Glade, B) Snapper Creek, C) Matheson Hammock.

of the water table from canalization, this glade was seasonally hydrated and was one of a series of 'transverse' glades that conveyed overflow water from the greater Everglades ecosystem toward Biscayne Bay (Figure 1). Although separated from Biscayne Bay by a narrow rock 'barrier' ridge (Figure 2), the presence of a mangrove wetland seaward of Deering Glade strongly suggests the construction of a 'delta' from water either overtopping or flowing through the barrier ridge. The early settlers cut a canal through this ridge in 1899 allowing water to more easily flow from the glade to the bay. In Sapper Creek to the north, the pre-development transverse glade also ended at the barrier ridge. Remnant wetland vegetation, such as

Pond Apple and Leatherfern within Deering Glade, provides support that standing water was a common feature of these lowlands. Both Snapper Creek and Cutler Canals now incise deep channels through the glade and the barrier ridge.

The spatial arrangement of the barrier ridge, the 'uplands' that are inland of the ridge, and the transverse glades are interpreted to be the product of a late Pleistocene (MIS 5e) tidal barrier-bar-belt system. In this context, the glades were shallow subtidal channels and the landward shoals were comprised of herringbone cross-bedded öolites (Halley et al., 1977). These channels and shoals were scoured into or deposited upon, respectively, a restricted platform inland of the Key
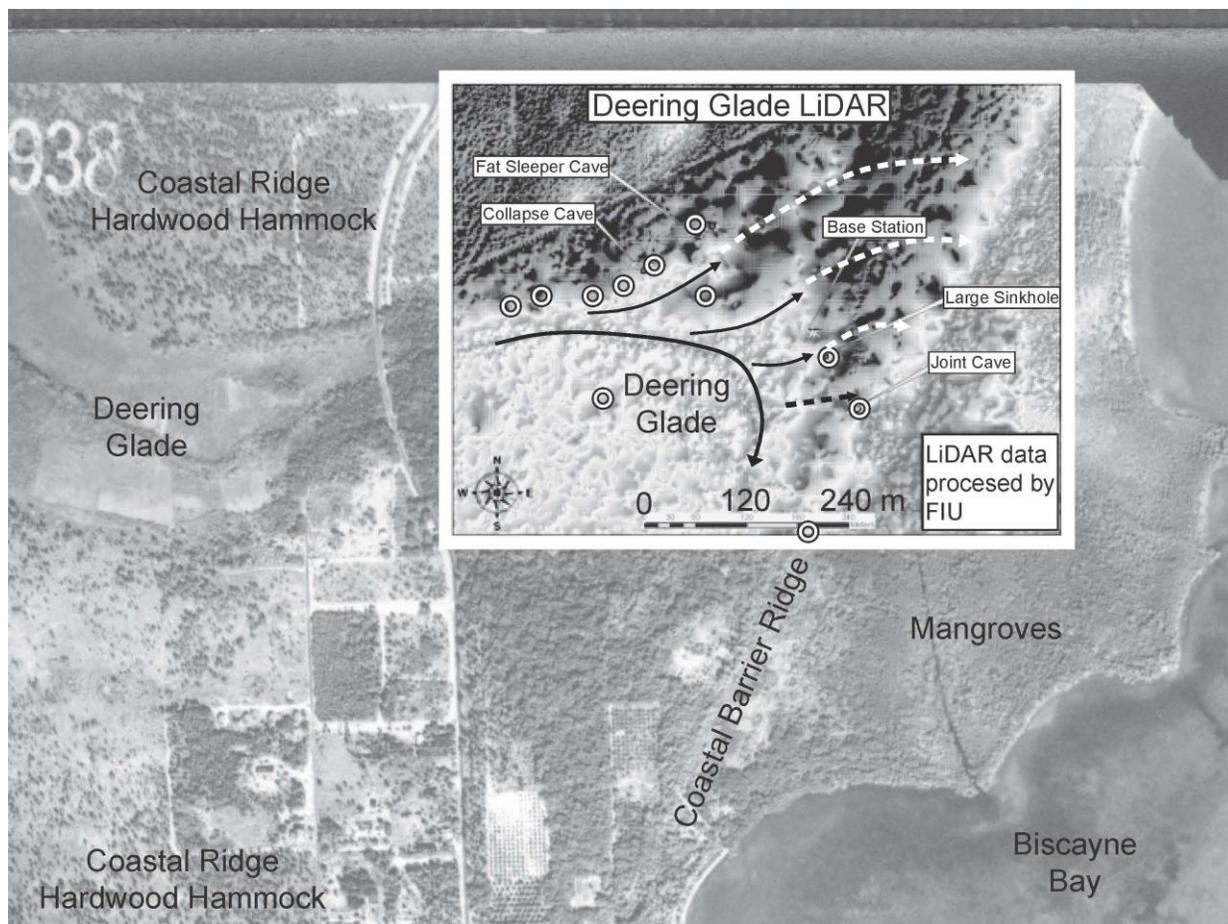
Figure 2. Historic 1938 aerial photo that is partly overlain with LiDAR data within the northern half of Deering Glade. Darker colors in the LiDAR map refer to higher elevations. Caves are indicated by open circles. Historic surface-water flow is shown by solid arrows. Hypothesized groundwater flow paths are illustrated in dashed arrows. The coastal barrier ridge and mangrove delta are both clearly visible in the imagery.

Largo barrier reef complex that was rich in burrowing *Callianasid* sp. shrimp that developed a strong *Ophiomorpha* ichnofabric (Curran, 2007) within the host öo-peloidal grainstone (Figure 3). Rapid deposition of the öolite bars is evidenced by the trace fossil *Conichnus conicus* and limited bioturbation. Once established, the tidal channels supported biostromes of mega-demosponges (Cunningham et al., 2007). Toward the end of MIS 5e, the barrier-bar ridge was accreted to the margin of the öolite shoals, occluding the outlets to what would become Snapper Creek and Deering Glade. Collectively, the tidal barrier-bar-belt system, and the *Ophiomorpha* facies comprise the Miami Limestone (Halley et al., 1977).

Caves and Karst

Between 2006 and 2012, we surveyed ten caves within the Atlantic Coast Ridge in Miami-Dade County, Florida, USA. These comprise a subset of the 20 features identified by Alan Cressler in his 1993 publication *Caves of Dade County, Florida* (Cressler, 1993). Seven of these caves are within Deering Glade. One is on University of Miami property near Snapper Creek. Another is within Camp Owassa-Bauer Park. The last is within Everglades National Park (Florea and Yuellig, 2007). Our database includes GPS locations for at least seven more caves that are not yet surveyed (Figure 1). These caves are a small subset of karst
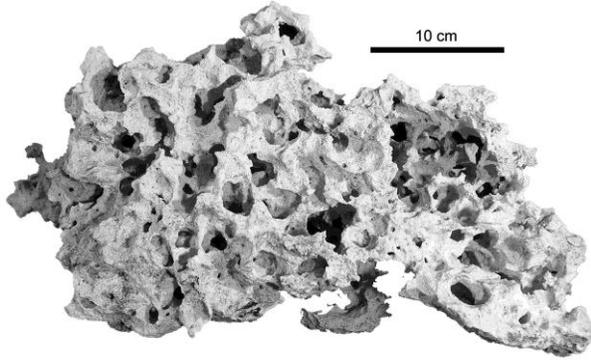
Figure 3. Photo of Ophiomorpha sp. *ichnofabric in the MIS 5e Miami Limestone. Surveyed caves are vertically restricted to this facies (photo by Kevin Cunningham).*

features within the Biscayne aquifer at the surface, within core, and detected by geophysical methods. Cunningham and Florea (2009) summarize of the types and spatial distribution of karst of southeast Florida.

The GPS data (Figure 1), cave maps (Figure 4), and petrographic studies along the north scarp of Deering Glade all suggest that the caves are geographically restricted to the glade margin and largely confined to stratiform high-permeability zones associated with the *Ophiomorpha* ichnofabric—the 'razor rock' of Cressler (1993). To date, our survey of these caves are restricted to the glade margin with horizontal openings to the north scarp and cylindrical pits open to the hammock surface (Figure 4); the physical size of these caves quickly diminishes below human dimensions. LiDAR data and the surface survey associate these caves with re-entrants in the glade scarp (Figures 2 and 5).

Deering Glade Rehydration Plan

Post-development canalization of the greater Everglades ecosystem resulted in at least two meters of water level reduction. This combined with pumping in the Biscayne aquifer resulted in saltwater intrusion along the coastline of Biscayne Bay (Renken et al., 2005). As of 1995, the greatest saltwater intrusion was present along the Miami River and the area south of Homestead and the least

intrusion surrounded Deering Glade (Renken et al., 2005, Figure 55). Control structures installed along canals have helped, but for decades Deering Glade and the caves in along the glade margin were relatively dry.

In 2010, under an interagency agreement with the South Florida Water Management District, Miami-Dade County, and the US Army Corps of Engineers, construction began on the Biscayne Bay Coastal Wetlands Project. This project is one element of the larger Comprehensive Everglades Restoration Plan (CERP). Phase I included the Deering Estate Flow-way designed to convey fresh water between the C-100 spur canal and Deering Glade. The design of the project includes a pump house and retention basin (Figure 5) constructed at the end of the C-100 spur canal. When water levels reach a specified height, water from the canal is pumped to the head of Deering Glade. To help retain water and return the glade to pre-development conditions, the historic cut in the barrier ridge was blocked.

Of relevance to the efficacy of this rehydration project is the flow of the freshwater through the glade-margin karst. Considering the permeability of the *Ophiomorpha* ichnofabric and the caves formed within this facies, it is a reasonable to question whether the glade could ever hold standing water. Our survey of caves only addresses the scope of pore spaces with an entrance and of human size. However, we know from our surveys that these caves are stratiform and laterally continuous at sizes below human scale. We also know nothing of the potential for karst features below the soil horizon within the glade.

In this study we present initial findings from two DC Electrical Resistivity Tomography (ERT) transects collected in Deering Glade. This geophysical method is commonly used to detect air-filled or water-filled voids in the subsurface (Zhou et al., 2002). One particularly useful advantage of this geophysical technique in this geologic setting is the ability to distinguish between strata saturated with freshwater and those saturated with saltwater

(e.g., Schneider and Kruse, 2005). Another is that it can discriminate between geologic media of different densities and mineralogical compositions. The goal in this was to see how far the karst penetrates into the glade margin, to see if detectable karst features exist below the glade, and to determine whether saltwater underlies this portion of Deering Glade. Each is an important consideration in the ultimate success of the rehydration project.

METHODS

ERT transects were collected on March 5–6, 2012 using a AGI Super Sting R1/IP with an array of 28 passive electrodes used in a dipole-dipole configuration (Figure 6). Using this configuration, one dipole (*AB*), with an electrode separation of *a*, serves as a current loop and the second dipole (*MN*), also with an electrode spacing

of *a*, measures the potential difference at some distance *na* away from that current loop, where *n* is an integer. Using the derived equation of electric potential in a uniform half space,

$$V = \frac{I\rho}{2\pi r} , \qquad [1]$$

where *V* is potential, *I* is current, *r* is the distance from the electrode, and ρ is the resistivity of the material, we can derive the relationship for the apparent resistivity in the dipole-dipole system, given by

$$\rho = -\frac{\pi a n(n+1)(n+2)}{I}\Delta V , \quad [2]$$

where *ΔV* is the voltage measured across the *MN* dipole. It is important to note that the apparent

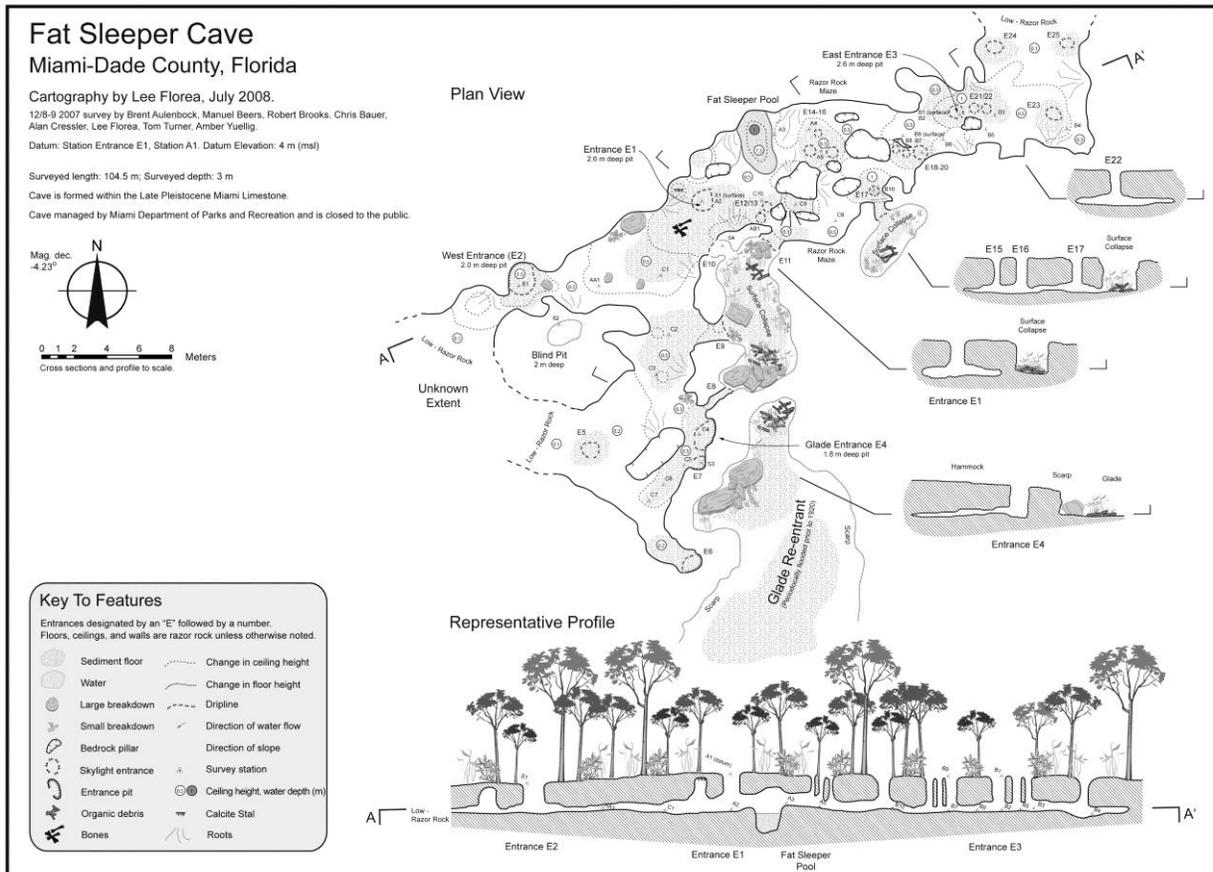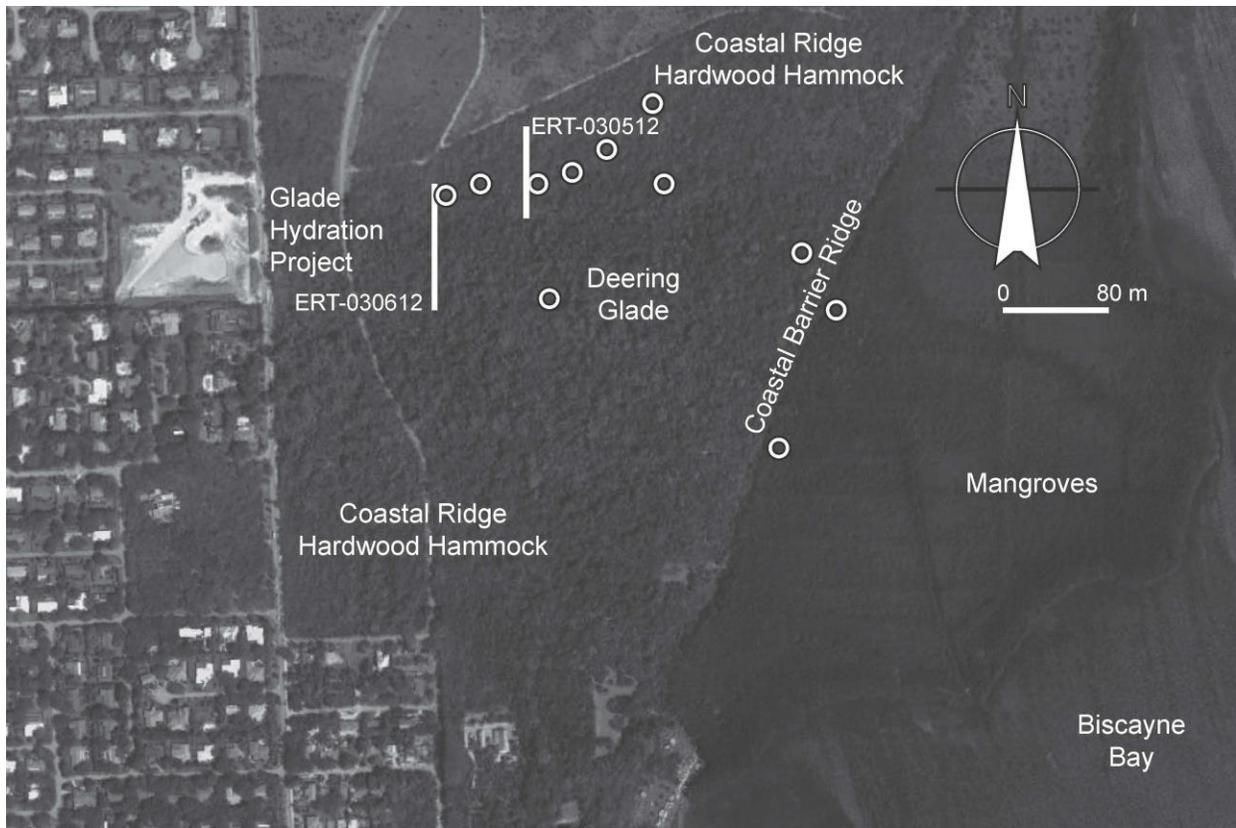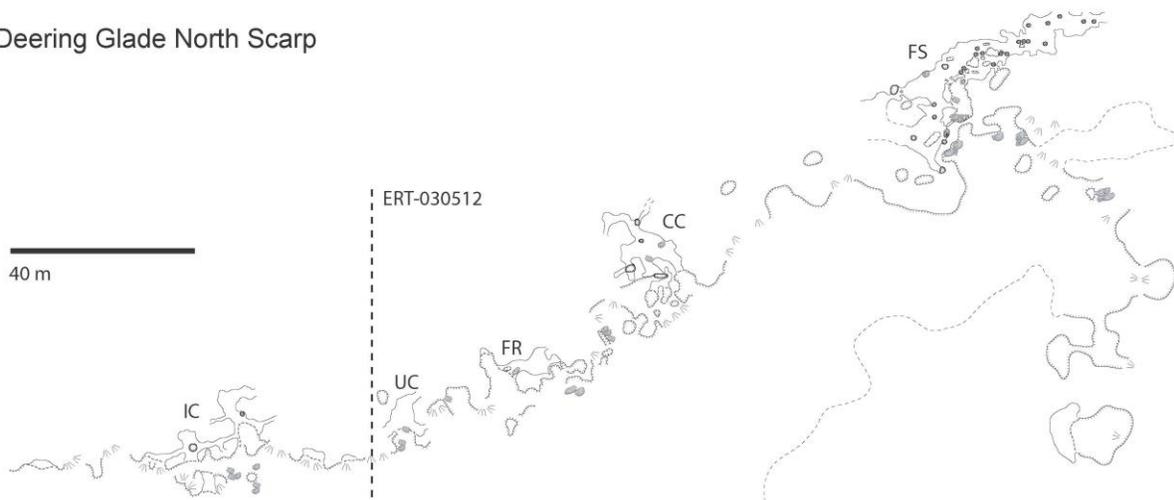*Figure 4. Map of Fat Sleeper cave in both plan and profile view.*

Figure 5. Top) Recent Google Earth image illustrating the location of the Deering Glade Flow-way retention basin. Caves are shown as open circles and ERT transects are shown by solid white lines. Bottom) Map of the north scarp of Deering Glade showing the location of caves (labeled by letter codes) and the glade edge ERT transect.

resistivity computed by equation [2] is an average of the earth resistivity along the entire path of the current loop. It does not represent the actual resistivity at a point beneath the earth surface. To model the resistivity at a point, a mathematical

inversion of the data is optimized against a forward model of the inverted data.

At Deering Glade, the first transect (ERT030512, Figure 5) comprised a 46-m 'roll-along' survey from the glade interior across the
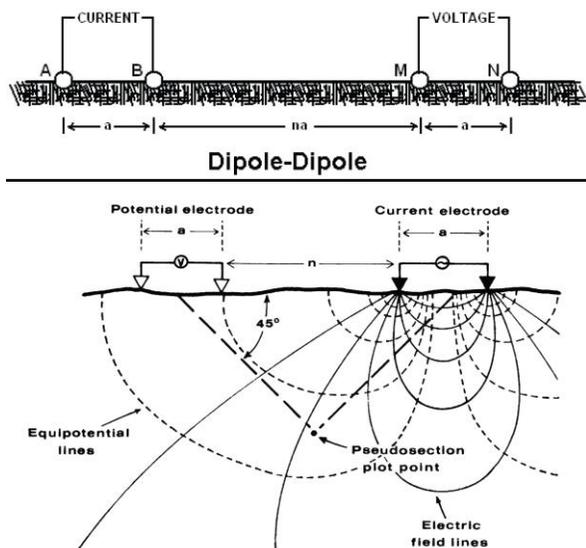
Figure 6. Dipole-dipole electrode configure ation used in ERT transects. A and B are current electrodes. M and N are potential electrodes (images from http://www. microgeo.com/detailed_discussions/dm3.html, accessed 12/02/2012).

north scarp. In this transect, we used one-meter electrode spacing ($a = 1$ m) with a 10-electrode overlap between the two segments. In the second transect (ERT030612, Figure 5), we spanned the glade using a 5-m spacing ($a = 5$ m) for a 112-m-long transect. Terrain files were collected for each transect that record the elevation of each electrode with respect to modern sea level. Our first and second transects 'see' to a depth of approximate 9 m and 27 m below modern sea level (bmsl), respectively.

Using Earth Imager 2D software by AGI, three cross-sections were generated for each ERT transect: measured apparent resistivity pseudo-section, inverted resistivity section, and calculated apparent resistivity pseudo-section. The measured apparent resistivity pseudo-section is a display of the field measurements of apparent resistivity. The inverted resistivity section is the model of the subsurface resistivity distribution. The calculated apparent resistivity pseudo-section is the forward model of apparent resistivity from the final iteration of the inverted data. For these data, we set the

number of iterations to eight or until the RMS error between the field data and forward model dropped below 5%.

RESULTS

The apparent resistivity pseudo-section, inverted resistivity section, and calculated apparent resistivity pseudo-section for the north scarp of Deering Glade (ERT030512) are shown in Figure 7. The inversion model took 6 iterations to reach a RMS of 3.74%. Modeled resistivity values are partly stratified with values of more than 1,000 $\Omega\cdot$m at elevations above the base of the scarp and generally less than 500 $\Omega\cdot$m below the elevation of the glade. Three anomalies have resistivity values approaching 10,000 $\Omega\cdot$m and suggest the presence of air-filled voids from the glade margin to a distance of 40 m along the transect. The lowest value of 27.1 $\Omega\cdot$m is within the range of rock saturated with freshwater. The location of these lowest values is adjacent to anomalies with high values of modeled resistivity. Such paired anomalies are common artifacts in Earth Imager 2D when sequential iterations within the inversion model attempt to reconcile strong contrasts in resistivity such as between a void and surrounding rock.

The apparent resistivity pseudo-section, inverted resistivity section, and calculated apparent resistivity pseudo-section for the longer transect across Deering Glade (ERT030612) are shown in Figure 8. The inversion model took 6 iterations to reach a RMS of 4.28%. The modeled resistivity is again stratified with values greater than 1,000 $\Omega\cdot$m largely restricted to the north scarp except for two anomalies below grade that are likely artifacts of the inversion model. The lowest resistivity values are concentrated near the channel within the glade and within an anomaly below the channel at a depth of approximately 12 m bmsl; however, values of modeled resistivity below 100 $\Omega\cdot$m are widespread at depths less than 8–10 m bmsl. Modeled resistivity values are generally higher (>200 $\Omega\cdot$m)
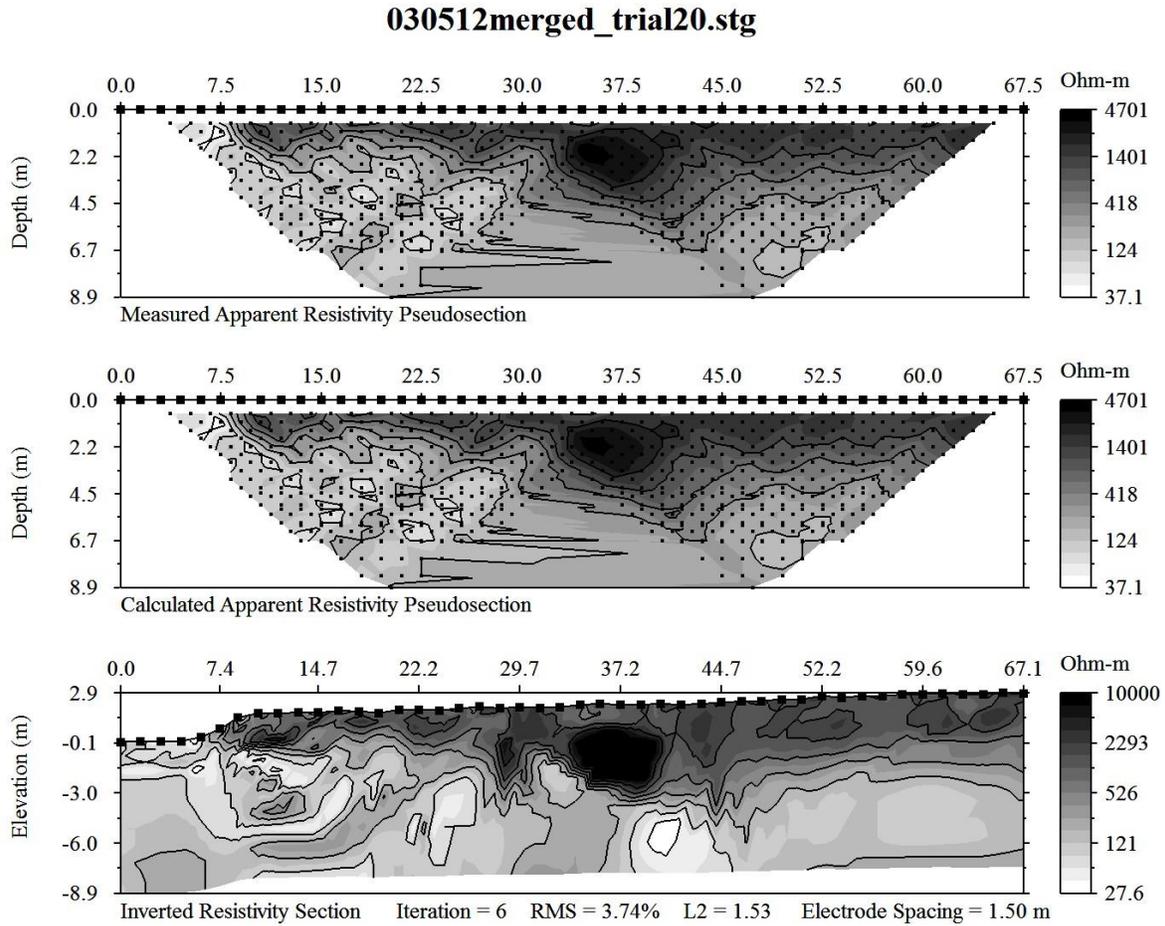
030512merged_trial20.stg

Figure 7. Measured apparent resistivity pseudo-section (top), inverted resistivity section (bottom), and calculated apparent resistivity pseudo-section (middle) for the glade edge ERT transect. Darker values correspond to higher values of resistivity. The high resistivity anomalies likely correspond to air-filled voids.

from 8–10 m bmsl to the base of the section at approximately 27 m bmsl.

DISCUSSION

Glade-Margin Karst

In the inversion model from the glade-margin transect (LF030512, Figure 7), modeled resistivity values greater than 1,000 Ω·m are a clear sign of a vadose zone of relatively dry limestone north of the glade scarp (Telford et al., 1990). In the inversion from glade transect (LF030612, Figure 8), the vadose zone in the north scarp is still visible. The three high-resistivity anomalies in the glade-margin transect are likely air-filled caves. The largest of the three anomalies centered at a distance of 37 m from the beginning of the transect correlates to an observed vertical pipe near the transect that opens into a void of unknown size or lateral scope. When overlain on the survey data from the north scarp, the anomalies generally align with the SW-NE trend of surveyed caves in the glade margin (Figure 9). This is also the approximate distance from the scarp edge beyond which vertical pipes into caves and surveyed cave passages are not observed. Considering the alignment, the shape, and the linearity of some cave passages along this trend, it is possible that this represents fracture traces that act as a preferred flow path for water leaving the glade.
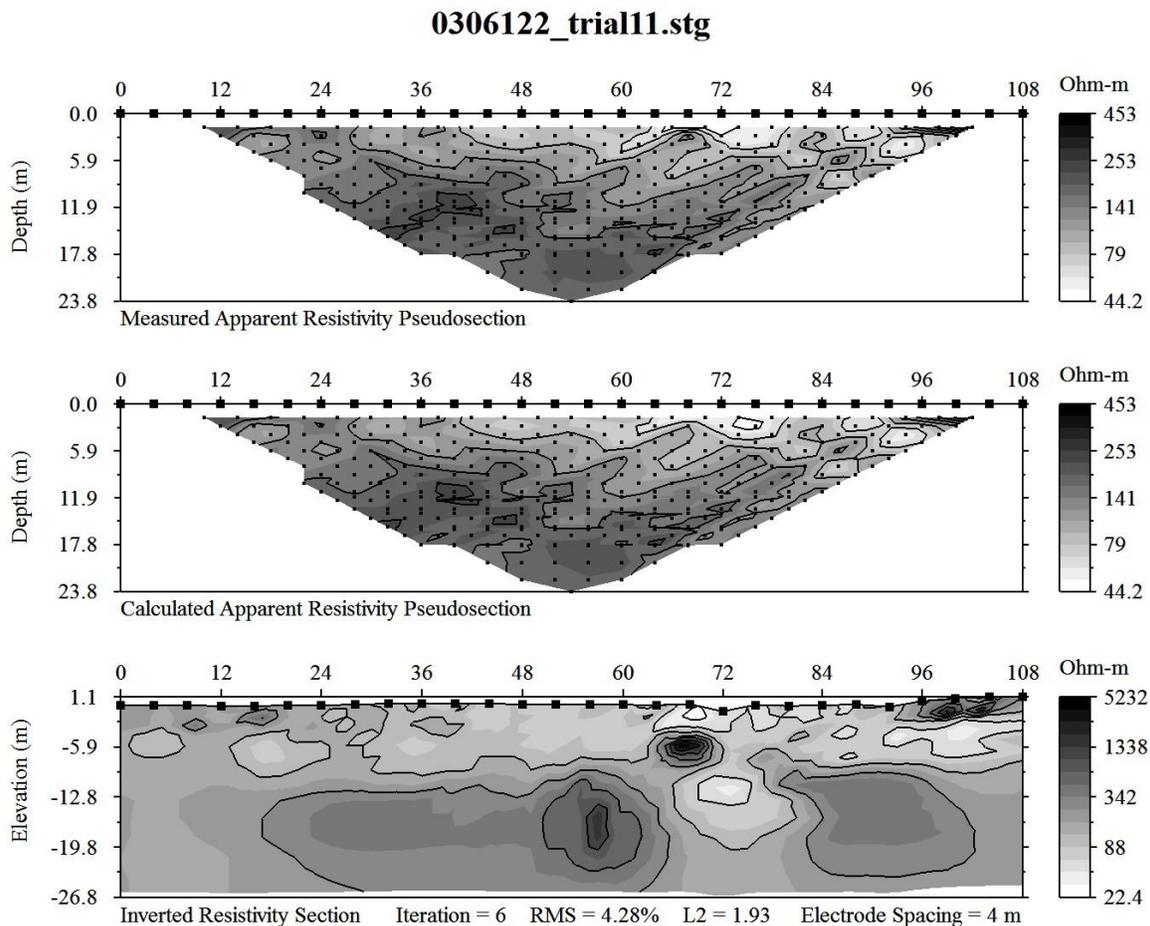
195

0306122_trial11.stg

Figure 8. Measured apparent resistivity pseudo-section (top), inverted resistivity section (bottom), and calculated apparent resistivity pseudo-section (middle) for the glade ERT transect. Darker values correspond to higher values of resistivity. The low resistivity anomaly likely corresponds to a water-filled void beneath the glade channel. Nearby high resistivity anomalies are possibly artifacts from the inversion model.

In contrast to the north scarp of Deering Glade, the southern glade margin has a gradual slope and lower values of modeled resistivity (Figure 8). Upon closer observation, the southern margin is highly dissected. The one intact cave surveyed in the southern part of the glade (Figure 2), is enclosed within a low 'mesa' of intact bedrock with a 'caprock' of herringbone crossbedded öolites. The terrain surrounding this cave is a jumble of bedrock blocks moved by excessive root wedging and tree throw. It is quite possible that this portion of the glade represents a mature-stage karst within the inside of the glade meander where widespread lateral dissolution of the *Ophiomorpha*

ichnofabric resulted in progressive collapse of the öolite overburden. Meeder and Harlem (2012) evoke this process in a recent abstract and argue that these caves represent one stage in the lateral growth of transverse valleys in the Atlantic Coastal Ridge. The role tree roots have upon the evolution and modification of these karst systems remains an unstudied phenomena.

Another potential interpretation is that these glade-margin caves represent the enlargement of preferential pathways that convey freshwater through the ridge to Biscayne Bay during periods of glade hydration. Certainly historical and ecological evidence exists of higher-than-present water levels
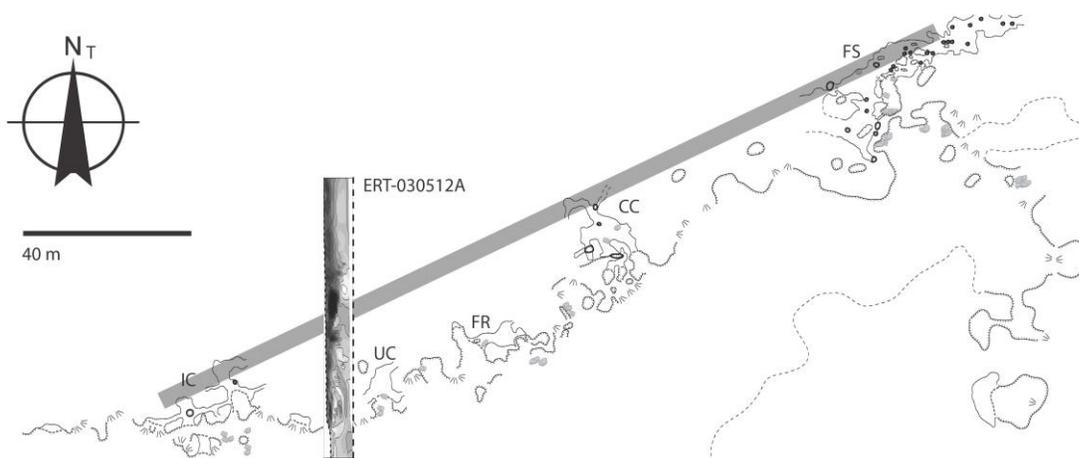
196

Figure 9: Map of the north scarp of Deering Glade showing the location of caves (labeled by letter codes). The glade edge ERT model is overlain at the location of the transect. The gray bar illustrates the alignment between mapped caves and voids identified using ERT.

in Deering Glade and more broadly within the transverse glades of the Atlantic Coastal Ridge. Ponding water behind the barrier ridge in Deering Glade would have developed a hydraulic gradient with fractures and the exceptional permeability of the *Ophiomorpha* ichnofabric focusing groundwater flow. The extremely high surface area to volume ratio of the touching-vug porosity created by the *Ophiomorpha* ichnofabric could promote rapid dissolution along these stratiform flowpaths. Near-coastal circulation of saltwater may have also enhanced dissolution along mixing zones and can explain some morphologic aspects of these caves, such as globular chambers, bedrock pillars, and low height-width ratios. However, the historic data and out ERT transects suggest the mixing zone is considerably below the position of these caves. Regardless of origin, these caves likely formed in a short timeframe, either during the Holocene when the surface hydrology of the modern Everglades evolved or during the initial regression of the MIS 5e highstand, and are an important agent of geomorphic change in south Florida.

Glade Hydration and Stratigraphic Architecture

Interestingly, the ERT data in both transects have values greater than what would be expected within media saturated with brackish or saline waters. At one level this is surprising given the proximity to the coastline and the widespread saltwater intrusion in southeast Florida. On the other hand, freshwater discharge to Biscayne Bay was enormous in pre-development time—there are photos of freshwater 'boils' in the middle of the bay used to resupply ships. As recently as 1995 saltwater intrusion near Deering Glade was less than elsewhere along the Atlantic Coastal Ridge (Renken et al., 2005, Figure 55). At Deering Estates today, there are small springs adjacent to the barrier ridge that discharge slightly brackish waters. Thus, it appears that, even today, the seepage face for freshwater is wide and the saltwater-freshwater interface is below the depth modeled using these ERT data.

There is some evidence in Figure 8 that freshwater from the Deering Estate Flow-way, operational for a short period before these ERT transects were collected, is helping to re-hydrate the base of the glade and the glade channel. While no standing water was observed, modeled resistivity values near the channel are generally less than 50 $\Omega \cdot m$. It would be an interesting study to repeat these ERT transects during various seasons and hydration states once the Flow-way becomes fully operational.

In addition to the air-filled caves in the scarp margin, the modeled resistivity data also

suggest the presence of a freshwater-filled void below the glade channel at an elevation of 12 m bmsl. Interestingly the elevation of this void is similar to the most common depth of water filled caves in other portions of the Florida platform (Florea et al., 2007), the Bahamas (Lundberg and Ford, 1994), and the Yucatan Peninsula (Smart et al., 2006). Meeder and Harlem (2012) suggest that features of this type may represent conduits conveying water from the Everglades toward Biscayne Bay.

The glade ERT transect generally conforms to a three-layer resistivity model with a high-resistivity vadose zone in the hardwood hammock and a less resistive layer overlying a more resistive layer elsewhere in the model (Figure 8). Both of these layers conform to limestone saturated with freshwater. The change in resistivity with depth potentially represents a geologic contact between highly permeable and less permeable bedrock between 8–10 m bmsl and may correlate to contact between the MIS 5e Miami Limestone and older carbonates of the Pleistocene Ft. Thompson Formation. Cunningham et al. (2004) place this contact at an elevation of 4 m bmsl at a distance of four miles west of Deering Glade. The depth to this contact generally increases toward the shore. While this runs counter to the traditional model of increasing permeability in older carbonates at depth presented in Vacher (1988), infiltrating non-carbonate sediments occluded the touching-vug porosity in the Ft. Thompson Formation prior to the deposition of MIS 5e carbonates (Cunningham et al., 2008).

CONCLUSIONS

Cave survey combined with modelled resistivity measurements using ERT support that karst solution within Deering Glade of the Atlantic Coastal Ridge is geographically restricted to the glade margin and largely confined to stratiform high-permeability zones associated with biogenic macroporosity. The ERT model specifically identifies what may be air-filled caves within the vadose zone of the adjacent hardwood hammock that occur along a linear trend with existing survey data. In contrast, the ERT model and survey data reveal a highly dissected southern glade margin created by excessive root wedging and tree throw. Below the glade channel, a low-resistivity anomaly potentially represents a cave filled with fresh groundwater. An increase in resistivity at 8–10 m bmsl may represent the contact between the MIS 5e Miami Limestone and older Pleistocene carbonates. No evidence of saltwater intrusion currently exists in the ERT data to a depth of 27 m bmsl.

ACKNOWLEDGMENTS

REFERENCES

Cressler, A., 1993, The Caves of Dade County, Florida: Georgia Underground, v. 30, no. 3, p. 9-16.

Cunningham, K.J., and Florea, L.J., 2009, The Biscayne Aquifer of Southeastern Florida, *in* Palmer, A., and Palmer, M.V. eds., Caves and Karst of America: National Speleological Society, pp. 196-199.

Cunningham, K.J., Sukop, M.C., Huang, H, Alvarez, P.F., Curran, H.A., Renken, R.A., and Dixon, J.F., 2008, Prominence of ichnologically influenced macroporosity in the karst Biscayne aquifer: Stratiform "super-K" zones: GSA Bulletin, v. 121 no.1-2, p. 164-180.

Cunningham, K.J., Rigby, J.K., Wacker, M.A., and Curran, H.A., 2007, First documentation of tidal-channel sponge biostromes (upper Pleistocene, southeastern Florida): Geology, v. 35, p. 475-478, dio: 10.1130/G23402A.1.

Cunningham, K.J., Wacker, M.A., Robinson, E., Gefvert, C.J., and Krupa, S.L., 2004, Hydrogeology and ground-water flow at Levee 31N, Miami-Data County, Florida, July 2003 to May 2004: U.S. Geological Survey Scientific Investigations Map I-2846.

Curran, H.A., 2007, Ichnofacies, ichnocoenoses, and ichnofabrics of Quaternary shallow-marine to dunal tropical carbonates: a model and implications: *in* Miller, W., III ed., Trace fossils: concepts, problems, prospects: New York, Elsevier, p. 232-247.

Florea, L.J., Vacher, H.L., Donahue, B., and Naar, D., 2007, Quaternary cave levels in peninsular Florida: Quaternary Science Reviews, v. 26, p. 1344-1361.

Florea, L., and Yuellig, A., 2007, Everglades National Park—surveying the southernmost cave in the United States: Inside Earth, v. 10, no. 1, p. 3–5.

Halley, R.B., Shinn, E.A., Hudson, J.H., and Lidz, B.H., 1977, Pleistocene barrier bar seaward of ooid shoal complex near Miami, Florida: American Association of Petroleum Geologists Bulletin, v. 61, p. 519-526.

Hoffmeister, J.E., Stockman, K.W., and Multer, H.G., 1967, Miami Limestone of Florida and its recent Bahamian counterpart: Geological Society of America Bulletin, v. 79, p. 175-190.

Lundberg, J., and Ford, D.C., 1994, Late Pleistocene sea level change in the Bahamas from mass spectrometric U-series dating of submerged speleothem: Quaternary Science Reviews, v. 13, no. 1, p. 1-14, dio: 10.1016/0277-3791(94)90121-X.

Meeder, J., and Harlem, P., 2012, Karst control of the Biscayne aquifer groundwater flow patters. Geological Society of America Abstracts with Programs, v. 44, no. 7, p. 206.

Renken RA, Dixon J, Koehmstedt J, Ishman S, Lietz AC, Marella RL, Telis P, Rogers J, and Memberg S., 2005, Impact of anthropogenic development on coastal ground-water hydrology in southeastern Florida, 1900–2000: US Geological Survey Circular 1275.

Schneider, J.A. and S.E. Kruse, 2005, Assessing natural and anthropogenic impacts on freshwater lens morphology on small barrier islands: Dog Island and St. George Island, Florida: Hydrogeology Journal, v. 14, p. 131-145, doi: 10.1007/s10040-005-0442-9, 2005.

Smart, P.L., Beddows, P.A., Coke, J., Doerr, S., Smith, S., and Whitaker, F.F., 2006, Cave development on the Caribbean coast of the Yucatan Peninsula, Quintana Roo, Mexico; *in* Harmon, R.S., and Wicks, C.M., eds., Perspectives on Karst Geomorphology, Hydrology, and Geochemistry—A Tribute Volume to Derek C. Ford and William B. White: Geological Society of America Special Paper 404, pp. 105–128.

Telford, W.M., Geldart, L.P., and Sheriff, R.E., 1990, Applied Geophysics (2nd ed): Cambridge University Press, New York.

Vacher, H.L., 1988, Dupuit-Ghyben-Herzberg analysis of strip-island lenses: Geological Society of America Bulletin, v. 100, p. 223-232.

Zhou, W., Beck, B.F., and Adams, A.L. 2002, Effective electrode array in mapping karst hazards in electrical resistivity tomography: Environmental Geology, v. 42, p. 922–928, doi: 10.1007/s00254-002-0594-z.